Laser Physics, Vol. 12, No. 7, 2002, pp. 1–9.

Femtosecond Photon Echo Spectroscopy in Single Laser Shot

A. Rebane[1], J. Callus[2], and O. Ollikainen[3]

[1] *Physics Department, Montana State University, Bozeman, MT, 59717, USA*

e-mail: Rebane@phvsics.montana.edu

[2] *Molecular Physics, Huygens Laboratory, University of Leiden, NL2300 The Netherlands*

[3] *Merkotex Inc., Männiku Tee 44, Tallinn, Estonia*

Received February 8, 2002

Abstract—We take advantage of extreme spatial thinness of 100-femtosecond pulse of an amplified femtosecond laser and measure for the first time the homogeneous spectrum of a strongly inhomogeneously-broadened solid with a single laser shot. This is achieved by combining causality-related diffraction asymmetry of two- and three-pulse photon echo with oblique excitation pulse wave fronts, which are creating a space-variable time delay. We show that by focussing the resulting photon echo image with a Fourier-transforming lens, we can directly record the autocorrelation function of the homogeneous spectrum. We measure the homogeneous line shape of dye-doped polymer at different temperatures, with spectral resolution up to 0.2 cm^{-1}, such that each measurement requires only one single laser pulse.

INTRODUCTION

First experimental demonstration of photon echo by Sven Hartmann in 1964 [1, 2] marked the beginning of a new era for high-resolution optical spectroscopy and for optical physics in general. Serendipity of this discovery comes from the fact that although photon echo was initially conceived theoretically as an extrapolation to optical resonance transitions of echo effects familiar from earlier radio-frequency magnetic resonance experiments [3, 4], the actual photon (light) echo signal first observed by Hartmann *et al.* turned out to provide an important benefit of a spatially-directed radiation [5], much like that of a coherent laser beam. Mostly due to this unique property, the effect of photon echo is widely used not only as a versatile spectroscopic tool, but has also opened new possibilities for laser-based applications such as optical storage, optical communications and many others.

One of the basic spectroscopic applications of photon echo consists in measuring of narrow homogeneous lines in the spectra of molecules and atoms in inhomogeneously broadened solids. At liquid helium temperatures, the inhomogeneous line width, Γ_{inh}, frequently exceed the homogeneous line width, Γ_{hom}, by as much as 10^5–10^8 times, which makes direct frequency domain measurement of homogeneous line shape impractical. Photon echo spectroscopy techniques consist in exciting an optical transition with a sequence of short pulses, and measuring the decay of the resulting optical coherence in time-domain [6–10]. The homogeneous line shape function can be extracted from the time-domain coherence decay data either by means of Fourier transformation or, in simple case of purely exponential decay, by virtue of inverse relationship between coherence decay time and homogeneous line width, $\Gamma_{hom} \sim 1/(\pi T_2)$.

In recent years, the accessibility of high power, wavelength-tunable ultrashort laser pulses has made it possible to extend the techniques of photon echo spectroscopy to new classes of materials with extremely rapid relaxation times, including semiconductors, large organic molecules and biological systems. Due to high time-domain resolution of femtosecond pulses, photon echo spectroscopy can provide information not only about the optical dephasing processes, but also about a variety of other important ultrafast phenomena, such as photochemical transformations, energy- and charge transfer between molecules, dynamics of vibrational excitations etc.

One of the goals of our research in recent years has been developing coherent transient techniques, which take advantage of special properties of ultrashort laser pulses such as broad spectral band width, high time resolution and high degree of localization of pulse intensity in space [11–15]. In the present paper we describe a novel approach to measurement of photon echo decay and associated homogeneous spectral line shape of organic dye molecules in polymer matrix in abroad range of temperatures with a spectral resolution up to 0.2 cm^{-1}. Our method is based on combining causality-related asymmetry of photon echo diffraction and extreme spatial thinness of femtosecond laser pulses. Two matching experiments are described, which both allow measuring the homogeneous spectrum within the time frame of a single laser shot In the first case, we make use of spatially-encoded time delay between two oblique plain wave front femtosecond pulses to excite

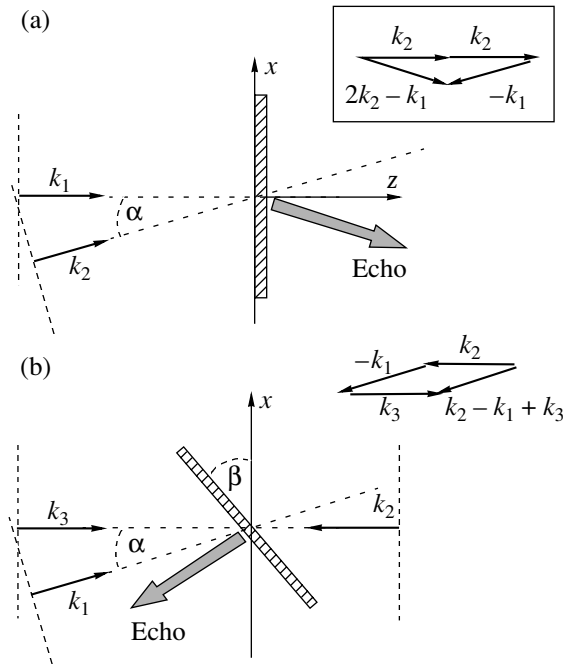

Fig. 1. Arrangement of excitation beams. Wave fronts are shown as dashed lines. Thin arrows show the propagation direction of the pulses. Thick arrow shows the direction of echo signal. (a) Two-pulse photon echo. The sample is parallel to the *x*-axis. (b) Three-pulse photon echo. The sample is tilted by angle β with respect to the *x*-axis. Inserts show corresponding wave matching diagrams.

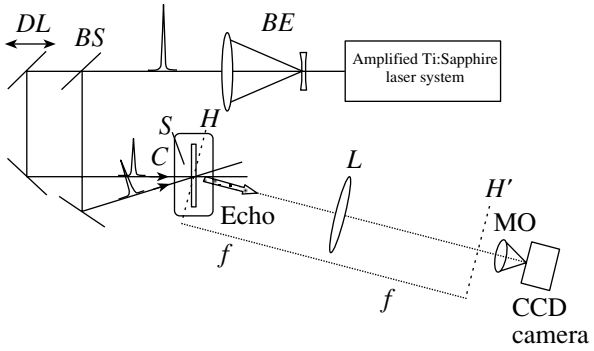

Fig. 2. Experimental set-up: BE, cylindrical beam expander; BS, beam splitter; *C*, cryostat; *S*, sample; DL, delay line; MO, microscope objective; *L*, cylindrical Fourier-transforming lens; *H*, front Fourier plane; *H*', back Fourier plane.

two-pulse photon echo, which yields autocorrelation function of the homogeneous spectrum in a single shot of a 100-fs laser. In the second experiment, single 100-fs pulse is devided into three oblique wave front pulses, applied from different directions, to excite three-pulse photon echo.

THEORETICAL CONSIDERATIONS

Figure 1(a) shows a plane wave front ultrashort pulse, with duration, τ_p, and carrier frequency, ν_0, propagating with wave vector, $\mathbf{k}_1 = \{0, 0, k\}$, and a second ultrashort pulse propagating in direction, $\mathbf{k}_2 = \{k\sin\alpha, 0, k\cos\alpha\}$, where α is angle between the two beams and $k = 2\pi\nu_0/c$. A sample comprising a thin plate of inhomogeneously broadened material is positioned at the origin perpendicular to *z*-axis. Two wave fronts meet at the origin at time $t = 0$. Due to the inclined geometry of the wave fronts, time delay between the pulses varies linearly with the distance *x* from the origin:

$$\tau(x) = \frac{x\sin\alpha}{c}. \quad (1)$$

Spatial properties of two-pulse photon echo [1, 2] are often described in terms of self-diffraction by a spatial-spectral grating of transient polarization in the medium, created by nonlinear interaction of the excitation pulses. The wave vector of such grating is, $\mathbf{K} = \pm(\mathbf{k}_1 - \mathbf{k}_2)$, where causality principle gives, plus (minus) sign, if the pulse with wave vector $\mathbf{k}_1$ arrives at the sample first (second). Note that in our special geometry, the temporal ordering of the pulses changes sign at the origin: for $x > 0$ the delay is positive and the echo propagates in the direction, $2\mathbf{k}_2 - \mathbf{k}_1$, whereas for $x < 0$ the delay is negative and the echo propagates in the complementary direction, $2\mathbf{k}_1 - \mathbf{k}_2$. In fact, we can imagine a distinct narrow line drawn through the origin and along the y-axis, where the echo amplitude switches its diffraction direction. **The width of this imaginary line depends on the pulse duration and the angle between the pulses**, $\Delta x = \tau_p c/\sin\alpha$. For $\tau_p =$ 100 fs and $\alpha \sim 10°$, we estimate $\Delta x \sim 0.17$ mm, which is much less than typical lateral dimension of our sample $d \sim$ 1–4 cm. Because causality-related switching of echo direction appears at this narrow line, we have given this feature earlier the name “time edge” [16].

In the following, both excitation pulses have the same temporal amplitude envelope profile, $E(t)$. Under such conditions, the photon echo signal is symmetrical in both diffraction directions.

The frequency-domain amplitude of the echo signal, emitted in the direction $2\mathbf{k}_1 - \mathbf{k}_2$, can be expressed as

$$P_{\text{echo}}(\nu, x) \propto E_2(\nu, x)\int_{-\infty}^{\infty} g_0(\nu'')\gamma(\nu - \nu'') \times \left[\int_{-\infty}^{\infty} E_1(\nu', x)E_2^*(\nu', x)\gamma(\nu' - \nu'')d\nu'\right]d\nu'', \quad (2)$$

where $g_0(\nu)$ is the inhomogeneous distribution function and $\gamma(\nu)$ is the homogeneous line shape function. Here

E_1 and E_2 are complex frequency-domain amplitudes:

$$E_1(\nu, x) = \int_{-\infty}^{\infty} E(t')e^{i2\pi(\nu-\nu_0)t'}dt';$$
$$E_2(\nu, x) = e^{i2\pi\nu\tau(x)}\int_{-\infty}^{\infty} E(t')e^{i2\pi(\nu-\nu_0)t'}dt'. \quad (3)$$

Typically, at least in a disordered polymer at low temperature, $\gamma(\nu)$ is a much narrower function than $g_0(\nu)$, and also much narrower than the femtosecond laser pulse spectrum, $E(\nu)$. Then, it is justified that we neglect the frequency dependence of the last two functions, and assume $g_0(\nu) \approx$ const., $|E(\nu)| \approx$ const. By substituting time delay (1), we express the echo amplitude as

$$P_{\text{echo}}(x) \propto e^{i2\pi\nu\tau}\int_{-\infty}^{\infty}\gamma(\nu-\nu'')\left[\int_{-\infty}^{\infty}e^{-i2\pi\nu'\tau}\gamma(\nu'-\nu'')d\nu'\right]d\nu''$$
$$= \int_{-\infty}^{\infty}\left[\int_{-\infty}^{\infty}\gamma(\nu'')\gamma(\nu''-\nu')d\nu''\right]e^{i2\pi\nu'\frac{x\sin\alpha}{c}}d\nu' \quad (4)$$

The basic physical meaning of Eq. (4) consists in dependence of the echo amplitude on the delay between the excitation pulses. Note that because of the special geometry of the beams, the dependence on the delay is transformed into dependence on the x-coordinate.

Let us assume now that the echo signal is measured with an image detector such as CCD camera. If the camera is focussed in the plane of the sample, $H(x)$, then the intensity of the image will be

$$I_{\text{echo}}(x) \propto \left|\int_{-\infty}^{\infty}\left[\int_{-\infty}^{\infty}\gamma(\nu'')\gamma(\nu''-\nu')d\nu''\right]e^{i2\pi\nu'\frac{x\sin\alpha}{c}}d\nu'\right|^2. \quad (5)$$

According to Eq. (5), the homogeneous spectrum is related to the measured image intensity via Fourier transform of auto-convolution function of $\gamma(\nu)$. To extract the information about the homogeneous spectrum, one has to perform inverse Fourier transformation of $I_{\text{echo}}(x)$. The most significant fact is, however, that in our case this transformation can be performed by purely optical means. For this purpose we position a cylindrical lens between the CCD camera and the sample plane $H(x)$, such that both distances are equal to the focal distance of the lens, f (Fig. 2). Intensity of the echo signal in the Fourier plane of the lens, $H'(\xi)$, is:

$$I_{\text{echo}}(\xi) \propto \left|\int_{-d/2}^{d/2}\left\{\int_{-\infty}^{\infty}\left[\int_{-\infty}^{\infty}\gamma(\nu'')\gamma(\nu''-\nu')d\nu''\right]e^{i2\pi\nu'\frac{x\sin\alpha}{c}}d\nu'\right\}e^{-i2\pi\frac{x\xi\nu_0}{cf}}dx\right|^2$$
$$= \left|\int_{-d/2}^{d/2}\left\{\int_{-\infty}^{\infty}\left[\int_{-\infty}^{\infty}\gamma(\nu'')\gamma(\nu''-\nu')d\nu''\right]e^{i2\pi\frac{x\nu_0}{cf}(\nu'\kappa-\xi)}d\nu'\right\}dx\right|^2, \quad (6)$$

where $\kappa = \dfrac{f\sin\alpha}{\nu_0}$. Here lateral dimension of the sample, d, defines the maximum "time window" of the Fourier transformation. If d is large, then Eq. (6) can be further simplified to give our final result:

$$I_{\text{echo}}(\xi) \propto \left|\int_{-\infty}^{\infty}\gamma(\nu')\gamma\left(\nu'-\frac{\xi}{\kappa}\right)d\nu'\right|^2. \quad (7)$$

Equation (7) shows that the intensity in the Fourier plane is directly proportional to the square of auto-convolution of the homogeneous spectrum, i.e. the image of the echo signal formed by the simple optical system gives directly the homogeneous spectrum of the medium, with out need for any data processing.

EXPERIMENTAL

Figure 2 shows the schematic of our experiment. The laser source was a regenerative-amplified Ti: Sapphire femtosecond laser system CPA-1000 (Clark MXR), with a variable repetition rate from 2Hz to 1 kHz. The laser pulses had duration of 100–120 fs, spectral width, $\Delta\nu_L$ = 7 nm, and energy 0.6–0.9 mJ. A cylindrical telescope beam expander (BE) increased the size of laser beam in x-direction from 10 mm to maximum of 40 mm. A 50% beam splitter (BS) divided the pulse equally between two beam paths. The angle of intersection between the beams at the sample was α = 10°, and the delay between the beams was adjusted such that the pulses overlapped temporally at the centre of the sample. The energy density of each beam at the sample was about 50 μJ cm^{-2} per laser shot.

Photon echo images were captured by using a gated CCD video camera 4 Quik 05 A (Stanford Computer Optics). The camera was used to image either the surface of the sample, $H(x)$, or the Fourier plane, $H'(\xi)$. In the latter case a cylindrical lens with focal length f = 350 mm was placed on the optical axis of the echo signal, and a 20× microscope objective was used to mag-

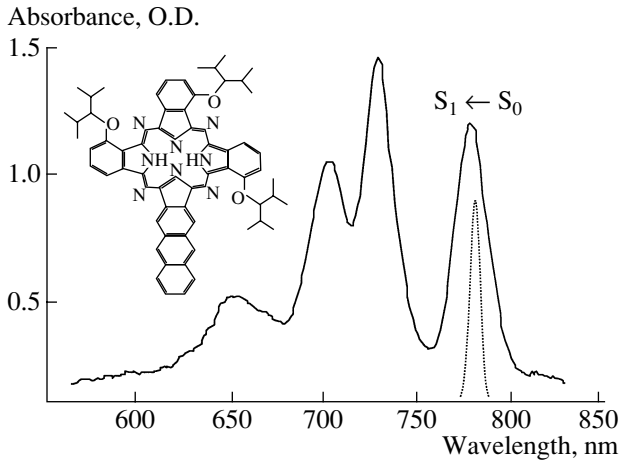

Fig. 3. Low-temperature absorption spectrum of anthtraceno-phthalocyanine in polyvinyl butyral film. Insert shows the structure formula of the molecule. Band at 780 nm corresponds to inhomogeneously broadened transition from ground singlet electronic state S_0 to the first excited singlet electronic state S_1, Dashed curve—intensity spectrum of the laser pulses.

nify the image in the back Fourier plane. The captured video images were digitized and processed by a computer.

In the arrangement for three-pulse photon echo, a third laser beam was propagated in negative *z*-axis direction by adding a second beam splitter and mirrors, as shown in Fig. 1b. The CCD camera along the Fourier imaging optics was repositioned to match the propagation direction of the three pulse photon echo. Combined energy density of all three beams on the sample was about 50–100 μJ cm^{-2} per laser shot.

The sample consisted of a 85 μm—thick polyvinylbutyral (PVB) polymer film activated with organic dye molecules at a concentration of about 10^{-4} mol/l. The lateral (*x* and *y*) dimensions of the illuminated area of the sample was 40 × 12 mm^2. The sample was contained in a **temperature-regulated liquid helium cryostat, with temperature variation** of the sample, T = 2–250 K. The optical density at the laser wavelength was O.D. = 1.0–1.5.

Figure 3 shows the absorption spectrum of a typical sample activated with anthraceno-phthahlocyanine (AnPc) molecules [17]. The wavelength of the laser pulses was tuned to the maximum of the inhomogeneously broadened $S_0 \leftarrow S_1$ absorption band in the range 770–780 nm, with a width, $\Gamma_{inh} \sim 22$ nm (370 cm^{-1}).

RESULTS AND DISCUSSION

Figure 4 shows images of two-pulse photon echo signal, which were obtained in a single laser shot at different sample temperatures. The left column show the actual two-dimensional spatial distribution of the echo signal intensity, recorded by CCD camera, and plotted as a function of the *x*-coordinate in the sample plane. In this experiment, according to relation (1), the illuminated length in *x*-direction, d = 17 mm, and the angle between the beams, $\alpha = 10°$, correspond to a maximum delay difference of about 10 ps. The right column shows the integrated intensity, which was obtained by summation of the image data points in vertical direction, and plotted as a function of the time delay between the two pulses.

The dependence of the intensity on the distance from $x = 0$ ($\tau = 0$) shows directly how the optical coherence of the $S_1 \leftarrow S_0$ transition changes with the time delay. The sharp intense feature at $x = 0$ ($\tau = 0$) is the so-called "time edge", which separates echo signal into two diffraction directions, depending on the temporal ordering of the excitation pulses. Note that to the left of the "time edge" the echo signal drops to zero due to causality principle [16, 17].

At T = 4.2–20 K, one can clearly distinguish two main contributions to the echo signal—one from zero-phonon line and the other from phonon side band [18]. At small delays, $\tau < 1$ ps, both contributions are present, whereas at larger delays, $\tau > 1$ ps, the phonon side band part vanishes and only the contribution from the zero-phonon line subsists. If the temperature increases to 50 K and above, then the zero-phonon line contribution fades away, and only the phonon side band persists. At even higher temperatures, up to room temperature, the optical dephasing time becomes comparable or even shorter man the duration of the excitation pulses. At room temperature the image consists only of the narrow vertical stripe at zero delay, where the two pulses overlap in time and space. In this case, the observed signal may be interpreted as self-diffraction from a spatial grating and is, therefore, a measure of the temporal coherence of the pulses, rather than of the optical dephasing in the medium.

We verified the accuracy of our present technique by a control experiment, where we compared the data in Fig. 4 with two-pulse photon echo decay measured by traditional step-by-step method [7, 9]. The step-by-step data is shown by dotted lines in the right column of Fig. 4, and it shows that disagreement between our method and the traditional methods is less than 10%. We underline that since the traditional method needs accumulation of at least several hundred of laser pulses, it is crucial that the sample always reappears in an exact initial state before every next laser pulse. Our new approach, however, accomplishes the whole measurement in the shortest possible time frame of one single laser pulse. This makes it feasible, at least in principle, measurement of optical dephasing in samples and systems, which change their state in an irretrievable manner, such as irreversible photochemical reaction, combustion, etc.

As discussed above, we can extract some qualitative features of the homogeneous line shape and the homo-

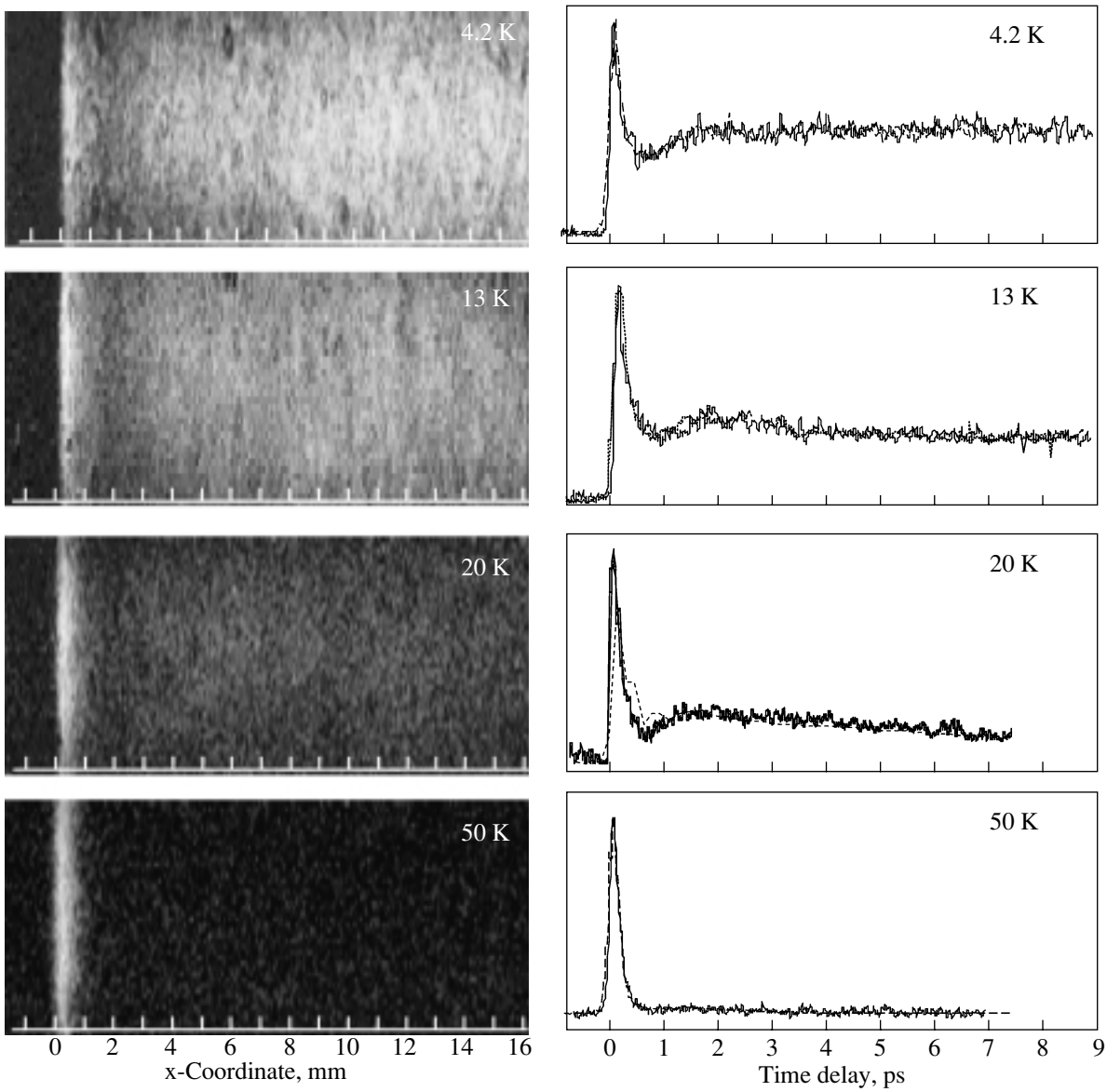

Fig. 4. Two-pulse photon echo detected in the plane of the sample. Left, photon echo image as recorded by CCD camera. Right column, vertically-integrated intensity data, plotted as a function of actual time delay between the pulses. Dashed curves are two-pulse echo intensity under similar conditions, but measured using conventional step-by-step delay variation method.

geneous dephasing just by considering the images in Fig. 4. However, to obtain quantitative information, it is necessary to perform numerical Fourier analysis of the experimental data [9]. Our next step is to perform the Fourier transformation function directly in the optical domain.

Figure 5 shows Fourier images of the single shot two-pulse photon echo signal. The left column show the two-dimensional spatial intensity, which was recorded by focussing the CCD camera in the back focal plane H' of the cylindrical lens, and is plotted as a function of the conjugated ξ-coordinate in the Fourier plane. According to relation (7), the meaning of the ξ-coordinate is actual optical frequency of the homogeneous line shape. Correspondingly, we have plotted the right column with the vertically-integrated intensity as a function of frequency with respect to the zero-phonon transition.

At low temperatures, T = 2–40 K, a distinctly narrow and intense line feature and a relatively much smaller side structure is seen at the centre of the image. With increasing temperature, the line gradually broadens and decreases in intensity, whereas the intensity and the width of the side structure increases. Eventually, above T = 100 K, the centre line and the broad

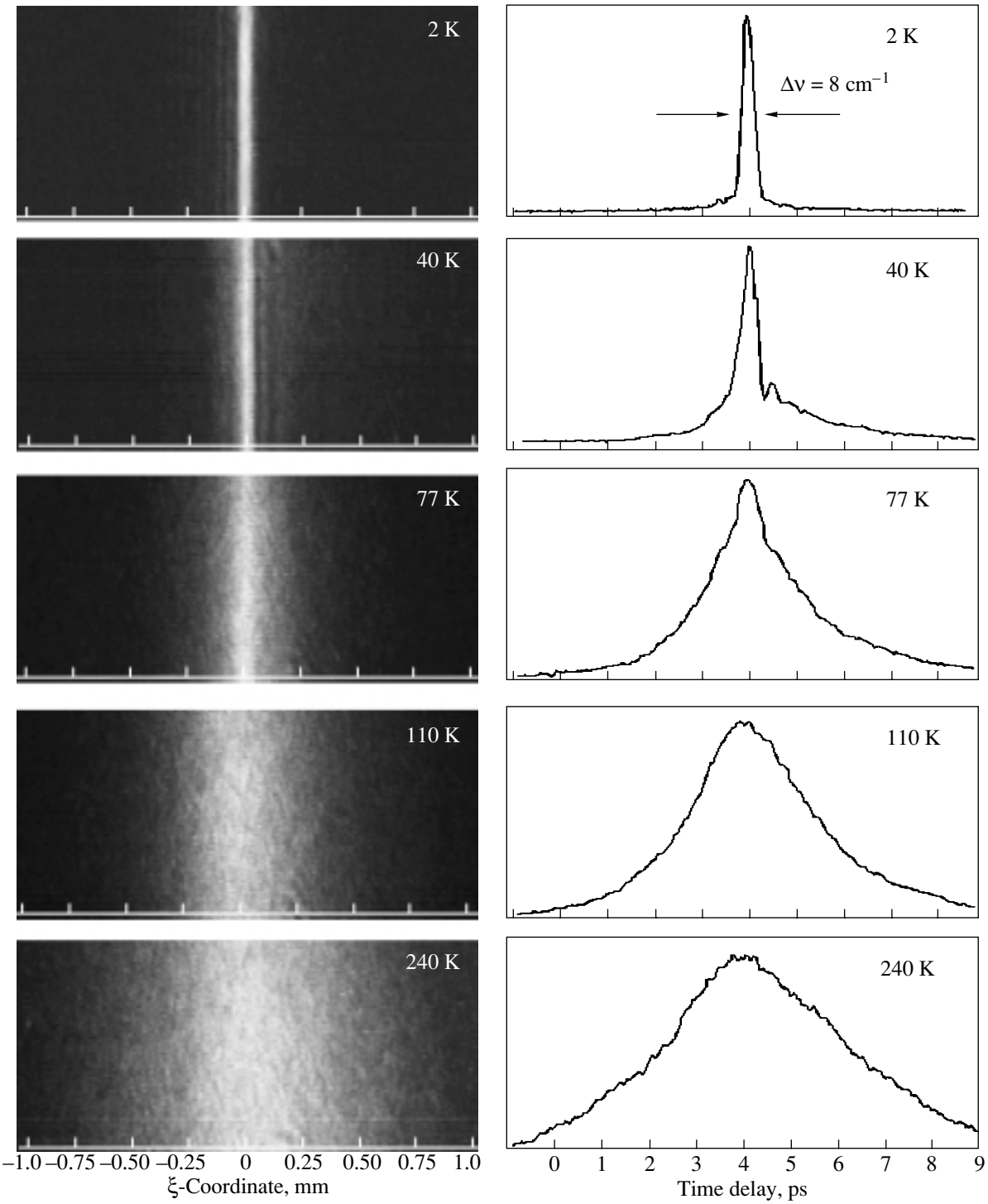

Fig. 5. Spatial Fourier-transform of two-pulse photon echo. Left column, two-dimensional image in actual spatial units. Right column, image data from the left integrated in vertical direction and normalized to the peak value. Note frequency units on the right-hand column.

structure merge into one broad feature, which makes them virtually indistinguishable from each other.

The appearance of the intensive line at lower temperatures corresponds well to the characteristic behavior of the homogeneous ZPL line, whereas the rapid growth of the broad side structures matches well the behavior of phonon side band at higher temperatures.

In a close analogy to conventional spectrometers, the ultimate frequency resolution of our single shot photon echo scheme results from inverse of the maxi-

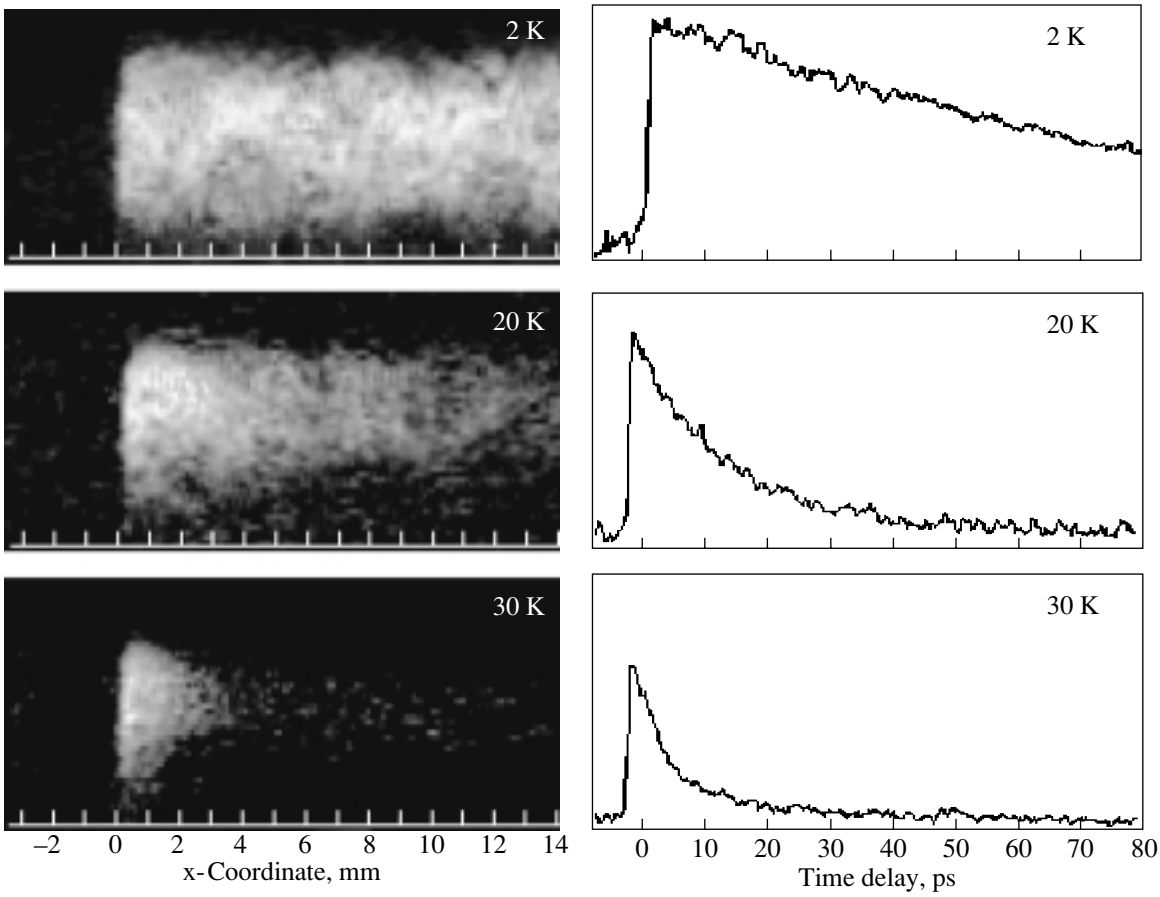

Fig. 6. Three-pulse photon echo detected in the sample plane. Left column, two-dimensional image in actual spatial units. Right column, image intensity from the left after integration vertical direction, *x*-axis is plotted in time delay units.

mum delay time window, $\tau_{max} = 10$ ps, and is estimated to be about 4 cm^{-1}. However, because of a limited reliability of the Fourier image, the actual resolution is about $\Delta\nu = 8$ cm^{-1}. Accordingly, the width of the narrow feature at low temperature reflects the resolution of the present experimental scheme, rather than the actual ZPL line width, which is known to be much narrower, $\Gamma_{ZPL} < 10^{-2}$ cm^{-1} at 2 K. On the other hand, at higher temperatures, our single shot data shows that the width of the phonon side band is about 20 cm^{-1}, and Debye–Waller factor is $\alpha_{DW} \sim 0.4$ at 77 K. which corresponds with values obtained from traditional persistent spectral hole burning measurement [17]. Thus, the image recorded by the CCD camera can indeed be interpreted quantitatively as the image of the homogeneous absorption spectrum of the resonantly absorbing molecules. The remarkable attribute of this result consists in the fact that the spectrum is measured within a single shot of a 100-fs laser pulse.

Our next step is to improve the spectral resolution by increasing the maximum delay time window. This is achieved by using a modified experimental arrangement, shown in Fig. 1b. In this case we apply three pulses, where the first and the second excitation pulses, k_1 and k_2, are directed from opposite sides of the sample. Additionally, the sample is tilted by angle $\beta = 40°$, with respect to the *x*-axis. As a result, the delay between the first and the second pulse varies on the sample in the range 0–160 ps, which is almost an order of magnitude more than in the previous scheme. The third pulse is sent from the same side as the first pulse, at an angle $\alpha = 5°$ relative to the *z*-axis. Furthermore, the third propagation direction is slightly tilled by a few degrees with respect to the *x*–*z* plane. As a result, the three-pulse photon echo is emitted also slightly out-of-plane, but to the other side of the *x*–*z* plane, which greatly facilitates the detection of the images.

Figure 6 shows images of three-pulse photon echo in a single laser shot, and at different sample temperatures. The left part shows again the two-dimensional intensity, and the right part shows the integrated one-dimensional intensity plotted as a function of the delay. Zero delay corresponds to temporal overlap of the first two pulses. The third pulse was always applied a few picoseconds after the second pulse. By comparing this result with Fig. 4, we notice that the contribution of the phonon side band, which was well pronounced in the two-pulse echo image, is nearly absent in the three-

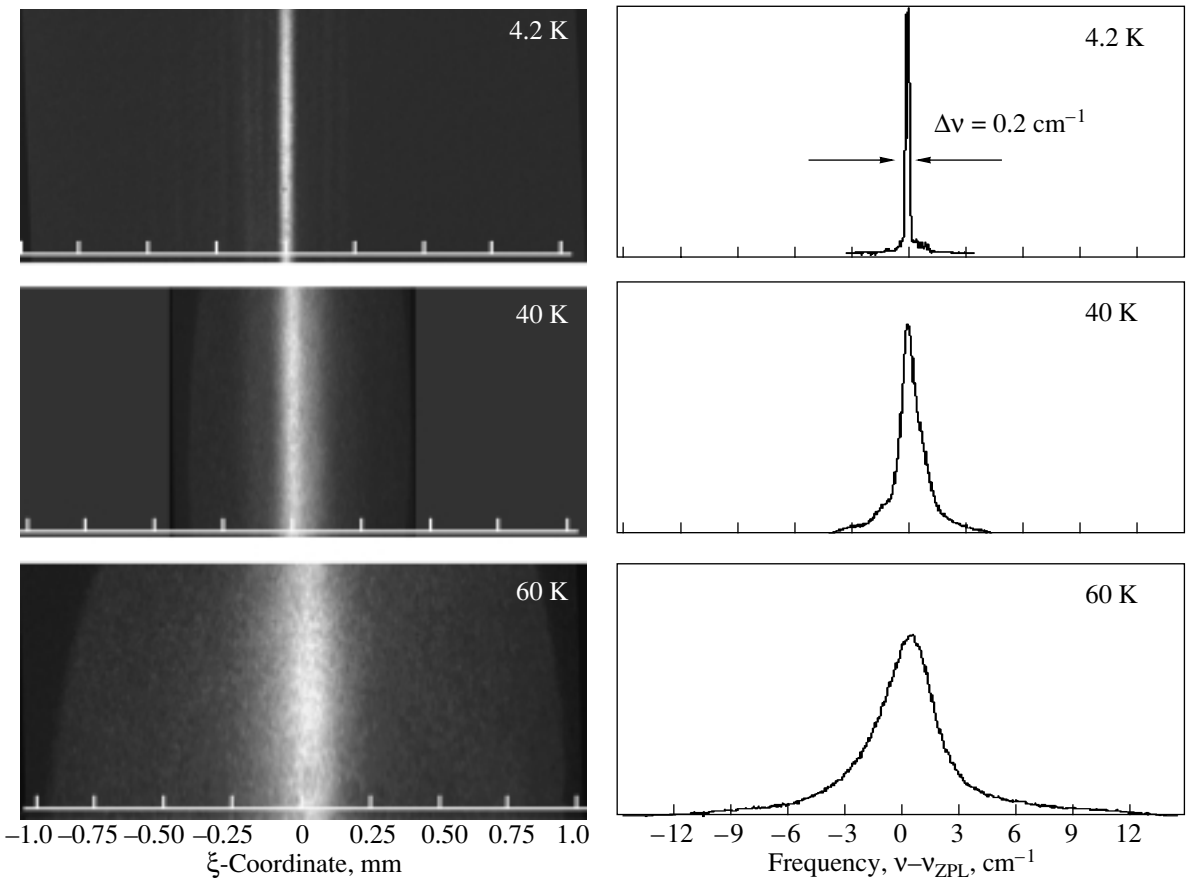

Fig. 7. Three-pulse photon echo signal Fourier plane *H*' at different temperatures. Left column, two-dimensional image in actual spatial units. Right column, vertically integrated image data from the left. Curves are normalized to the peak value and plotted in frequency units.

pulse photon echo image. This difference can be explained by the fact that two-pulse photon echo originates from non-equilibrium grating in polarization of the resonant transition, whereas the three pulse photon echo has also a major contribution from a grating in population [20, 21]. Since population relaxation time of phonon transition can be shorter than the few picoseconds time interval between the second and the third pulse, it is expected that phonon side band is less expressed in the three-pulse photon echo image. On the other hand, this effect facilitates following of ZPL to a higher temperature, than it was previously possible in the two pulse photon echo experiments.

Figure 7 shows three-pulse photon echo image Fourier-transformed with the cylindrical lens. In analogy to the above derivation of relation (7), one can easily obtain a similar expression describing the spectral image of homogeneous spectrum created by three pulse photon echo [22, 23]. Most important point here is, however, that data at 4.2 K shows a width of 0.2 cm^{-1}. This means that by using special illumination geometry we have achieved a ten-fold increase of the spectral resolution. Considering that the illumination is carried out with a single shot of a 100-fs laser pulse, with a spectral width of over 100 cm^{-1}, we think that this outcome is quite remarkable.

Finally, Fig. 8 summarizes the width of homogeneous spectrum measured by single shot three-pulse echo method in a broad range of temperatures between 2 K and 120 K. Each data point was taken under two different conditions—at 1 kHz laser pulse repetition rate (rectangles) and when the sample was illuminated only with one pulse at every given temperature (circles). The fact that higher repetition rate leads to a distinctly broader line width, can be explained by local heating of the sample due to accumulation of absorber energy. This underlines again the importance of measuring the spectrum in a single laser shot, such that no accumulated heating effects can occur.

In conclusion, we have shown how Hartmann's original photon echo experiments can be adapted by taking advantage of modern technology of high intensity femtosecond laser pulses, ú particular, we have demonstrated an experimental technique, which allows measuring the homogeneous spectral line shape in the presence of large inhomogeneous broadening by using just one single-shot of a femtosecond laser. We show

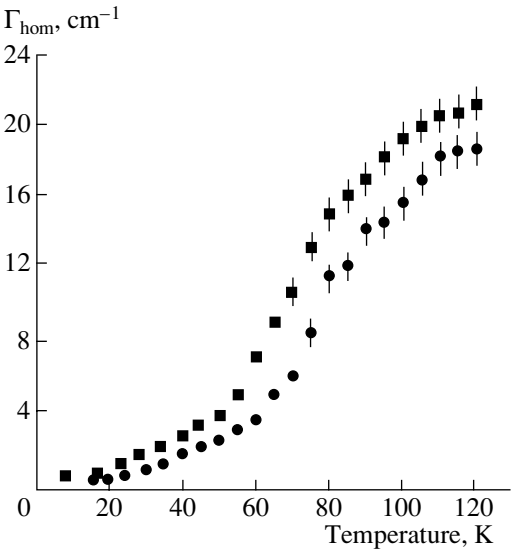

Fig. 8. Temperature dependence of homogeneous line width measured by single shot three-pulse photon echo. Each data point corresponds to a single laser shot. Circles, time interval between laser pulses more than 1 minute; squares, laser pulse repetition rate 1 kHz.

that by combining photon echo excitation with spatially-encoded time delay and all-optical Fourier-transformation, one can obtain a spatial photon echo image, which directly corresponds to the autocorrelation of the homogeneous absorption spectrum of the medium. We apply this method to measure homogeneous line shapes of dye molecules in polymer matrix in a broad range of temperatures and achieve a spectral resolution of 0.2 cm^{-1}. The fact that the whole measurement is accomplished in time frame of one single femtosecond laser pulse makes it feasible to study irretrievable irreversible processes such as ultrafast photochemical reactions, not accessible by conventional spectroscopic methods.

ACKNOWLEDGMENTS

The authors acknowledge the sponsorship by the Swiss Federal Institute of Technology (Zurich, Switzerland) and thank Prof. Ufs Wild for supporting these experiments. A. Rebane acknowledges the support by AFOSR Award F49620-01-1-0406.

REFERENCES

1. Kurnit, N.A., Abella, I.D., and Hartmann, S.R., 1964, *Phys. Rev. Lett.*, **13**, 567.
2. Kurnit, N.A., Abella, I.D., and Hartmann, S.R., 1966, *Phys. Rev.*, **141**, 391.
3. Feynman, R.P., Vernon, F.L., and Hellwarth, R.W., 1957, *J. Appl. Phys.*, **28**, 49.
4. Kopvillem, U.Kh. and Nagibarov, V.B., 1963, *Fiz. Met. Metalloved.*, **15**, 313.
5. Dicke, R.H., 1954, *Phys. Rev.*, **93**, 99.
6. Chandra, S., Takeuchi, N., and Hartmann, S.R., 1972, *Phys. Lett. A*, **41**, 91.
7. Chen, Y.C., Chiang, K., and Hartmann, S.R., 1980, *Phys. Rev. B*, **21**, 40.
8. De Silvestri, S., Weiner, A.M., Fujimoto, J.G., and Ippen, E.P., 1984, *Chem. Phys. Lett.*, **112**, 195.
9. Saikan, S., Nakabayashi, T., Kanematsu, Y., and Tato, N., 1988, *Phys. Rev. B*, **38**, 7777.
10. Zewail, A.H., Orlowski, T.E., Jones, K.E., and Godar, D.E., 1977, *Chem. Phys. Lett.*, **48**, 256.
11. Rebane, A., Kaarli, R., Saari, P., Anijalg, A., and Timpmann, K., 1983, *Opt. Commun.*, **47**, 173.
12. Saari, P., Kaarli, R., and Rebane, A., 1986, *J. Opt. Soc. Am. B*, **3**, 527.
13. Rebane, A., Aaviksoo, J., and Kuhl, J., 1989, *Appl. Phys. Lett.*, **54**, 93.
14. Schwoerer, H., Erni, D., and Rebane, A., 1995, *J. Opt. Soc. Am. B*, **12**, 1083.
15. Rebane, A., Drobizhev, M., and Sigel, C., 2000, *Opt. Lett.*, **25**, 1633.
16. Rebane, A., Ollikainen, O., Erni, D., Schwoerer, H., and Wild, U.P., 1995, *J. Lumin.*, **64**, 283.
17. Rebane, A. and Feinberg, J., 1992, *Nature*, **351**, 378.
18. Renge, I., Wolleb, H., Spahni, H., and Wild, U.P., 1997, *J. Phys. Chem.*, **101**, 6202.
19. Rebane, K.K., 1970, *Impurity Spectra of Solids* (New York: Plenum).
20. Mossberg, T.W., Kachru, R., and Hartmann, S.R., 1979, *Phys. Rev. A*, **20**, 1976.
21. Shtyrkov, E.I. and Samartsev, V.V., 1978, *Phys. Status Solidi A*, **45**, 647.
22. Ollikainen, O., Gallus, J., Wild, U.P., and Rebane, A., 1998, *Technical Digest of IQEC* (San Francisco), p. 227.
23. Gallus, J., 1999, *PhD Thesis* (ETHZ), no. 13249.

SPELL: devided, phthahlocyanine